Available online at www.sciencedirect.com
ScienceDirect
Journal of the European Ceramic Society 30 (2010) 113–118
www.elsevier.com/locate/jeurceramsoc

Effect of nano-AlN content on the microstructure and mechanical properties of SiC foam prepared by siliconization of carbon foam

Yu Yang [a,b], Quangui Guo [a,*], Xianda He [a], Jingli Shi [a], Lang Liu [a], Gengtai Zhai [a]

[a] *Key Laboratory of Carbon Materials, Institute of Coal Chemistry, Chinese Academy of Sciences, Taiyuan 030001, China*
[b] *Graduate University of the Chinese Academy of Sciences, Beijing 100039, China*

Received 16 November 2008; received in revised form 29 July 2009; accepted 6 August 2009
Available online 5 September 2009

Abstract

Mesophase pitch (MP) was doped by nano-AlN to produce carbon foams followed by liquid silicon infiltration to prepare silicon carbide foams. Experiments have been carried out to investigate the effects of nano-AlN doping on bending strength and thermal shock resistance of the silicon carbide foams. Microstructure observation and phase identification indicate that AlN doping strengthens the silicon carbide foams by grain refining and solid-solution reaction. With 13 wt.% of nano-AlN, silicon carbide foams were obtained with the highest quality in bending strength of 14.1 MPa, thermal shock resistance, and bulk density of 0.73 g/cm^3.

Keywords: SiC; Carbon; Thermal shock resistance; Strength; Oxidation resistance

1. Introduction

Ceramic foams such as SiC, TiC and Al_2O_3 are highly porous, low-density materials characterized by unique three-dimensional skeleton structure.[1] SiC foam is widely used as catalysis carriers, high temperature insulation materials and filters for hot gases and molten metals because of its excellent performance in strength, as well as shock and oxidation resistance at high temperature.[2,3]

Silicon carbide foams with bending strength of up to 2.87 MPa have been prepared from commercial SiC particles and polyurethane sponge by coating and sintering.[4] However, the covalent bonds in SiC are so strong that the sintering temperature is forced up to even higher than 2300 K although various additives such as boron, alumina and yttria have been used.[5,6] Since Aoki and McEnaney prepared SiC foams by adopting carbon foams as templates,[7] the template conversion method has attracted growing attention because of the easily accessible various templates and the realizable structure-design.[8–12] Recently, increasing interest has been drawn to the preparation of biomorphic porous SiC ceramics prepared by chemical gas-phase infiltration into various charcoal.[13–16] In contrast to all the work on the preparation of SiC foams, little has been done on mechanical property enhancement and microstructure modification.

Silicon carbide foams would be prepared by infiltration of a liquid silicon into the template carbon foams. The as-prepared foams would have uniform and controllable pore size. Moreover, this method is economically more attractive with respect to the low reaction temperature and the machinable template.

In the present study, silicon carbide foams with relatively high bending strength and good thermal shock resistance were prepared from mixtures of MP and nano-AlN particles, followed by foaming, carbonization, and infiltration of liquid silicon. Finally, a heat treatment was made on the resultant foams above 2173 K for 3 h in order to improve the solid solution of AlN in SiC. Nano-AlN as a solid solute in SiC could enhance the mechanical strength and thermal shock resistance of the silicon carbide foams.[18] Effects of nano-AlN content on the structure and performances of as-prepared silicon carbide foams were investigated.

2. Experimental procedures

2.1. Sample preparation

The Mitsubishi naphthalene based MP was used as the precursor for carbon foams. Nano-AlN particles with specific surface area of 85 m^2/g and mean particle diameter of 20 nm were added

* Corresponding author. Tel.: +86 3514184106; fax: +86 3514083952.
E-mail address: sea8011@163.com (Q. Guo).

0955-2219/$ – see front matter © 2009 Published by Elsevier Ltd.
doi:10.1016/j.jeurceramsoc.2009.08.006

into the melting MP at 570 K, followed by agitating and cooling. The grinded mixture was put in a pressure vessel and heated to 523 K at 4 K/min, and then heated to 723 K at 2 K/min under a pressure of 3 MPa in nitrogen atmosphere, finally held at 723 K for 4 h. The resultant foams were carbonized at 1273 K for 5 h at slow heating rates less than 15 K/h in argon atmosphere. The carbon foams with a dimension of 10 mm × 10 mm × 40 mm were put into graphite crucible and silicided via the infiltration of molten silicon at 1900 K in vacuum to obtain SiC foams. Samples were further heat-treated at 2173 K in argon atmosphere.

2.2. Sample characterization

The pore volume fraction of the resultant foams was calculated by the Archimedes method. The microstructures of foams were observed by scanning electron microscope (SEM) (JEOL JSM-6360LV). Three-point bending strength of each foam was measured by the CMT4303 universal material testing system with a crosshead speed of 0.5 mm/min, and the bending strength value (σ_f) was counted by $\sigma_f = 3PL/2wt^2$, where P is the fracture stress of the samples, L is the span, w and t were the width and the height of the samples, respectively.

Room temperature X-ray diffraction (XRD) measurements were conducted by a Brucker-AXS D8 Advance vertical $\theta/2\theta$ goniometer. The diffractometer utilized Cu Kα radiation (40 kV and 40 mA). The crystallite dimensions of foams were calculated by substitution of the 1 1 1 diffraction peak data into the Scherrer equation:

$$t = \frac{K\lambda}{B\cos\theta}$$

where t is the average crystallite size in the sample, λ is the X-ray wavelength (0.15406 nm), B is the breadth of the diffraction peak (full width half maximum), and 2θ is the diffraction angle, a K of 0.89 was chosen.

Oxidation resistance was characterized by thermogravimetric analysis (NETZSCH STA 409). The resultant foams were tested from room temperature to 1673 K at a heating rate of 3 K/min in flowing air. Thermal shock resistance of resultant foams was appraised by the analysis of bending strength decline of specimens after 10 water quenching cycles between 1173 K and room temperature.

3. Results and discussion

3.1. Effects of nano-AlN content on the bulk density and porosity of SiC foams and their templates

Fig. 1 shows the bulk density and porosity of silicon carbide foams and their templates as a function of nano-AlN content. Fig. 1a indicates that the bulk density of template carbon foams increases with the increase of nano-AlN content, but porosity shows a reverse tendency. As nano-AlN content increases, MP content decreases and viscosity of the molten MP increases,[19] which restrains the MP from decomposing[20] and makes it difficult for the bubbles to grow and combine.[21] When the addition amount of nano-AlN is above 17 wt.%, the agglomeration of

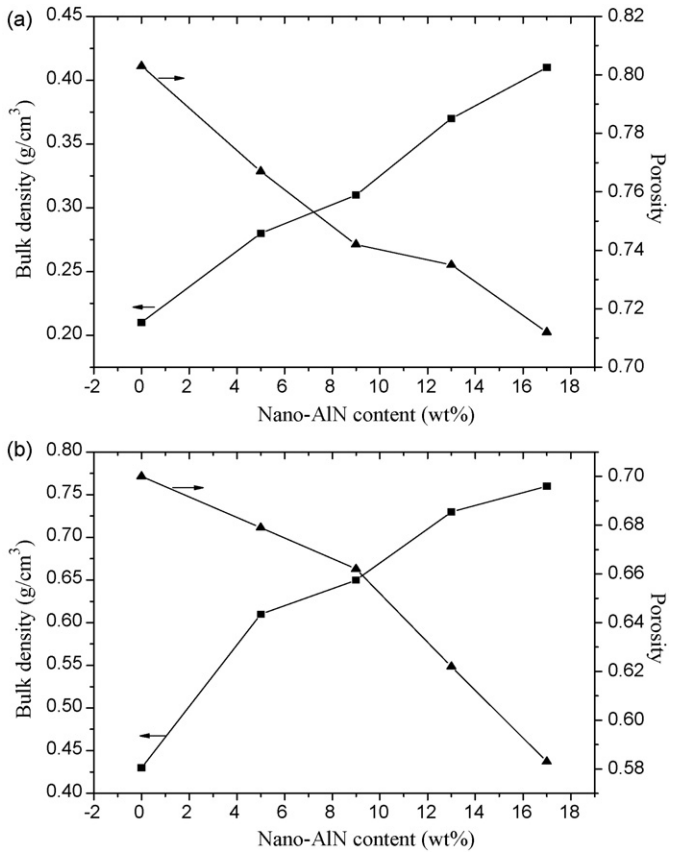

Fig. 1. Effects of nano-ALN content on the bulk density and pore volume fraction of SiC foams (b) and their precursors (a).

nano-AlN particles is aggravated and the molten MP phase is destroyed. As a result, carbon foams with uniform pore distribution could not be obtained. So carbon foams with addition amount of nano-AlN above 17 wt.% were not discussed in this paper. As shown in Fig. 1b, with the increase of nano-AlN, the variation of bulk density and porosity of silicon carbide foams presents the same trend as that of their templates. At the same time, the bulk density of the resultant foams becomes higher and the pore volume fraction becomes lower than that of carbon templates because of the change of carbon into silicon carbide by infiltration of the liquid silicon.

3.2. Microstructure

The effect of nano-AlN particles addition on microstructure of silicon carbide foams is shown in Fig. 2. Fig. 2a shows that SiC foam without nano-AlN addition has relatively loose cell walls with irregular grains. Grain refinement occurs by the addition of nano-AlN as demonstrated in Fig. 2b and c. Furthermore, the grains are in more regular shape and with uniform size, which is favorable to the densification of cell walls and struts in samples. However, excessive addition of nano-AlN would lead to particle agglomeration as marked by a white area in irregular shape in Fig. 2d.

Heterogeneous nucleation of nano-AlN in infiltration and solid-solution reaction in heat treatment are two important fac-

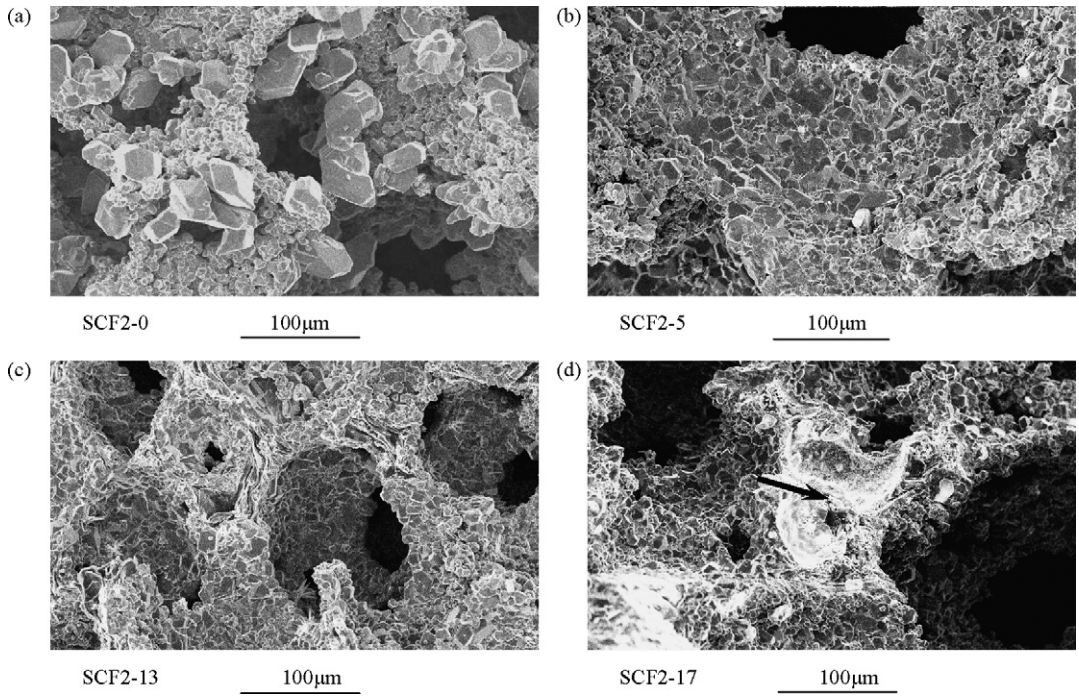

Fig. 2. Microstructure of SiC foams of SCF2 series (SCF2-0, 5, 13, 17, the addition amount of nano-AlN were 0, 5, 13, 17 wt.%).

tors for grain refinement. Ness and Page figured out the process of reaction sintering of C-Si is a resolving and secondary deposition process.[22] The solid-solution mechanism of AlN–SiC during the heat-treatment was also put forward by Zangvil and Ruh.[23] During the infiltration, nano-AlN as crystal seeds could accelerate the crystallization rate of SiC, which was in favor of the formation of fine grains. On the other hand, preferential diffusion of AlN on the surface of SiC grains occurs due to higher vapor pressure and diffusion rate of AlN compared with SiC in 2173 K. Thus the grain growth of SiC has been suppressed and the grain has been refined by secondary nucleation in the solid-solution reaction. So compared with SCF2-0, grains in SCF2-5, 13, 17 become evenly distributed and smaller.

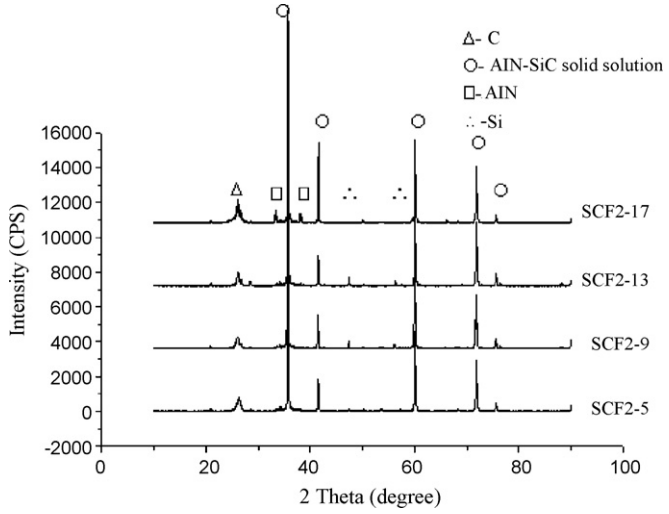

Fig. 3. XRD spectra of different SiC foams.

XRD patterns reveal that the SiC–AlN solid solution is the major phase with minor fraction of C (Fig. 3). As a result, when the nano-AlN addition amount is up to 17 wt.%, diffraction peak of residual AlN is detected as an indication of the uncompleted solid-solution reaction. In SCF2-5, 9, 13, AlN solid dissolves completely into SiC, which corresponds to the diffraction peak disappearance of AlN. However, excessive addition of nano-AlN would lead to particle agglomeration, which prevents AlN solid desolution in SiC and results in the residual AlN in SCF2-17. As listed in Table 1 the lattice constant (a) and the average crystallite size (t) for the resultant foams were calculated for different nano-AlN addition amounts. The gradual decrease of lattice constant with the AlN content increase as shown in Table 1 reveals that the lattice distortion of SiC increases with the solid-solution quantity increase of AlN. At the same time, the addition of nano-AlN particles reduces significantly the average crystallite size of SiC foams as demonstrated in Table 1.

3.3. Effect of nano-AlN content on the performances of SiC foams

3.3.1. Oxidation resistance

Fig. 4 describes the weight loss of different SiC foams heated from room temperature to 1673 K at a heating rate of 3 K/min in flowing air to test the oxidation resistance of the resultant foams. An obvious weight loss peak is observed in all samples between

Table 1
Lattice constant and average crystallite size of different samples.

	SiC	AlN	SCF2-5	SCF2-9	SCF2-13	SCF2-17
a (Å)	4.358	3.144	4.355	4.353	4.352	4.350
t (nm)	–	–	59.82	56.91	54.67	51.92

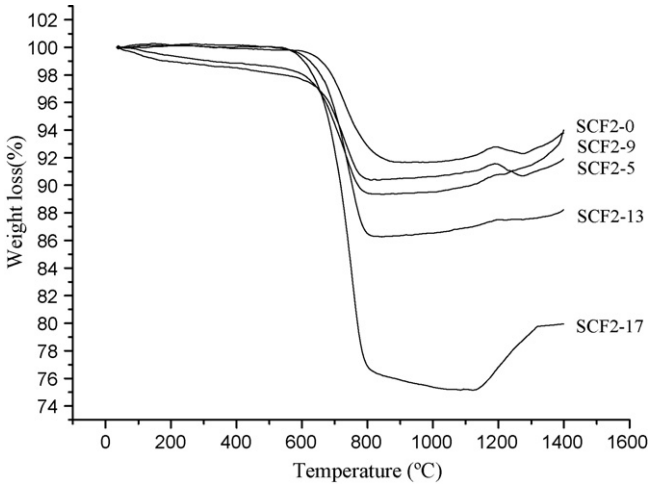

Fig. 4. Thermogravimetric curves of different samples.

873 and 1073 K due to the oxidation of residual carbon. Especially SCF2-17 has the maximum weight loss of 24% compared to other SiC foams. It is shown that SCF2-17 contains the most residual carbon after the infiltration of liquid Si, which is due to the close-pore increase with the AlN content increase. On the other hand, a slow weight gain appears at 1373 K in all samples due to the oxidation of a small amount of silicon carbide foam matrix. Both SiC and AlN exhibit excellent oxidation resistance because the oxide film prevents oxygen from infiltrating into the matrix during oxidation. However, the oxidation of residual carbon could destroy the SiC foam matrix and hamper the compact oxide film formation. It would aggravate the oxidation of the SiC foam matrix, which is also confirmed by more obvious weight gain of SCF-17 than that of other samples.

3.3.2. Bending strength

Fig. 5 shows bulk density and bending strength of silicon carbide foams as a function of nano-AlN content. Bulk density increases with the increase of nano-AlN addition amount. However, bending strength of silicon carbide foams firstly increases and then decreases with the increase of nano-AlN addition amount.

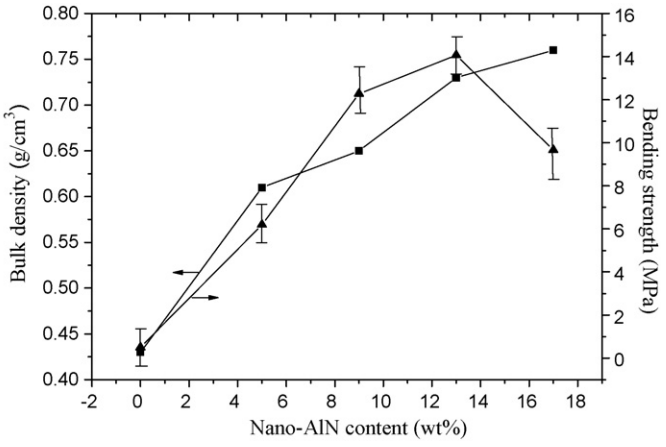

Fig. 5. Bulk density and bending strength of SCF2 series.

It is also shown in the previous studies[24,25] that the mechanical properties of open cell ceramic foams are complicated, which might depend on both bulk density and strut strength of foams. Based on the polycrystalline materials fracture rule, the strut strength of polycrystalline ceramic foams is thought to depend on intrinsic strength of material as well as average grain size. The mechanical strength equation derived for a model cubic open cell foam was put forward by Gibson and Ashby[25]:

$$\sigma = K\sigma_s \left(\frac{\rho_b}{\rho_s}\right)^{3/2}$$

where σ is the mechanical strength of the open cell foams, σ_s is the strut strength of foams, K was a constant, ρ_b and ρ_s were bulk density and strut density in foams, respectively.

Although the resultant foams showed a monotonic increase response in bulk density with the nano-AlN addition amount increase, effect of the nano-AlN addition amount on the strut strength of resultant foams is complex. For the SiC/AlN ceramic foam, strengthening mechanism is the combined action of the grain refinement and the AlN solid solution in SiC. As is known, both AlN dissolved in SiC and much grain boundary resulting from the grain refinement are defects in foam matrix, which would act as a nail to restrict cracks from developing and enhance the strut strength of resultant foams. However, as the nano-AlN addition amount is up to 17 wt.%, excessive residual carbon in SCF2-17 results in the decrease of bending strength. So bending strength of silicon carbide foams firstly increases and then decreases with the increase of nano-AlN addition amount.

3.3.3. Thermal shock resistance

Thermal shock resistance of the resultant foams was also appraised by the analysis of bending strength decline of specimens after 10 water quenching cycles between 1173 K and room temperature. As shown in Fig. 6, bending strength of specimens decreases in different degree after 10 water quenching cycles. At the same time, bending strength of specimens firstly increases and then decreases with the increase of nano-AlN addition amount independent of the thermal shock treatment.

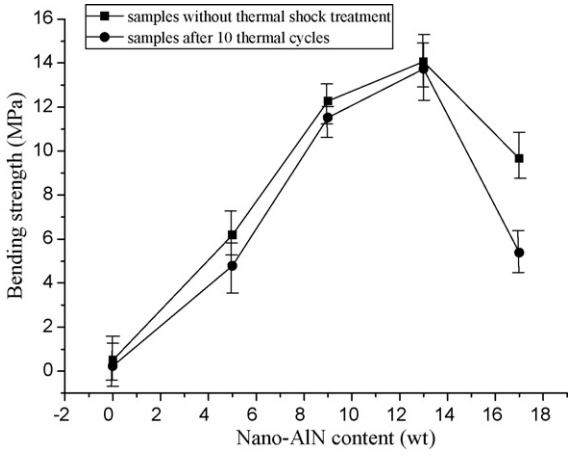

Fig. 6. Effect of nano-AlN content on thermal shock resistance of resultant foams.

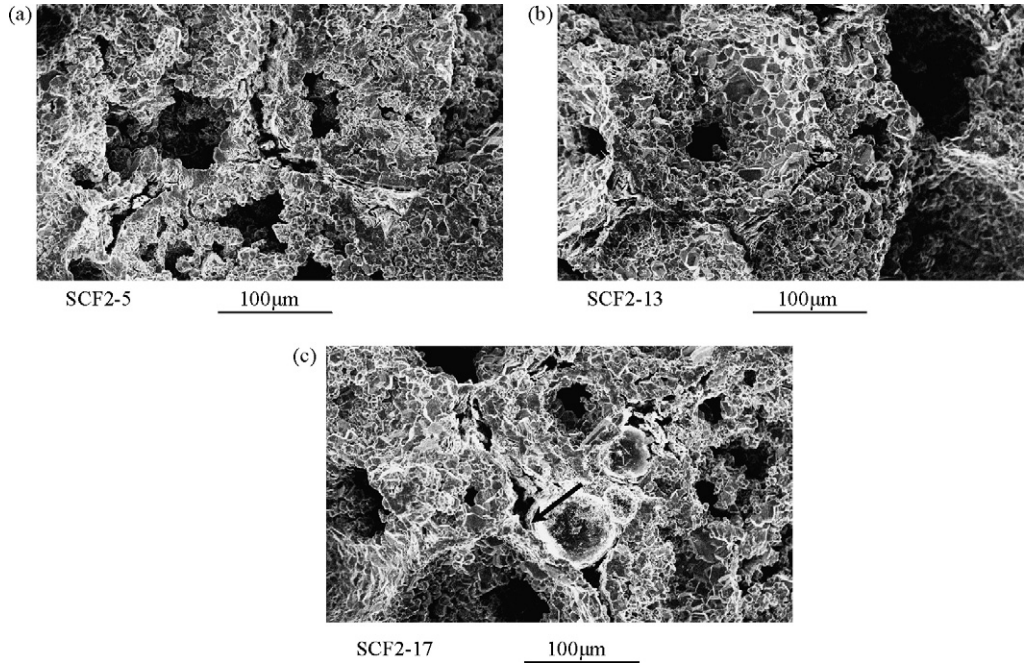

Fig. 7. SEM micrograph of the different SiC foams after 10 thermal shock cycles.

Table 2
Bending strength decline ratio (φ) of different samples.

	SCF2-0	SCF2-5	SCF2-9	SCF2-13	SCF2-17
φ	54%	22.6%	6.2%	2.3%	44.2%

Thermal stress and fracture theory put forward in previous paper[26] figured out cracks is a key factor of ceramic fracture when thermal stress is beyond mechanical strength of ceramic. So thermal shock resistance of ceramic materials depends mainly on its mechanical strength and thermal conductivity. As shown in Table 2, bending strength decline ratio (φ) of samples has a significantly decrease with the nano-AlN addition amount increase. As nano-AlN is added, bending strength of samples increases, which reduces crack generation, meanwhile, the grain refinement could effectively relieve crack propagation. Especially, as demonstrated in Fig. 7b almost no crack in SCF2-13 was observed. So the nano-AlN addition enhanced thermal shock resistance of SiC foams. However, excessive AlN addition would result in the increase of residual carbon and AlN in resultant foams, at the same time, cracks are more easily generated at the interfaces of SiC/C and SiC/AlN during thermal shock treatment because of the mismatch of thermal expansion coefficient, as demonstrated in Fig. 7c. So bending strength decline ratio of SCF2-17 was larger than that of SCF2-13.

4. Conclusions

The preparation and performances of silicon carbide foam with high bending strength and good thermal shock resistance were reported. It is illustrated that the addition amount of nano-AlN particles in carbon foam template could significantly affect the structure and performances of silicon carbide foams such as bulk density, porosity, cell microstructure, bending strength, and thermal shock resistance. The grain refinement and the solid-solution reaction with nano-AlN addition occur, which could significantly enhance bending strength and thermal shock resistance of resultant foams. However, excessive addition of nano-AlN would lead to particles agglomeration and the close-pore formation during molten MP foaming process, which is unfavorable for the improvement of mechanical strength and thermal shock resistance of resultant foams. Experimental investigation shows that an optimum amount of nano-AlN addition is 13 wt.% to achieve a bending strength of resultant foam of up to 14.1 MPa.

References

1. Zhang, Y. H., Microstructures and mechanical properties of silicon nitride bonded silicon carbide ceramic foams. *Mater. Res. Bull.*, 2004, **39**, 755–761.
2. Gómez de Salazar, J. M., Barrena, M. I., Morales, G., Matesanz, L. and Merino, N., Compression strength and wear resistance of ceramic foams–polymer composites. *Mater. Lett.*, 2006, **60**, 1687–1692.
3. Zhu, S. M., Ding, S. Q., Xi, H. A. and Wang, R. D., Low-temperature fabrication of porous SiC ceramics by preceramic polymer reaction bonding. *Mater. Lett.*, 2005, **59**, 595–597.
4. Liu, Y., Yao, X. M., Huang, Z. R., Dong, S. M. and Jiang, D. L., Preparation of high performance silicon carbide foam ceramics for filter of molten metal. *J. Chin. Ceram. Soc.*, 2004, **32**, 107–112.
5. Wang, Y. X., Tan, S. H. and Jiang, D. L., The effect of porous carbon preform and the infiltration process on the properties of reaction-formed SiC. *Carbon*, 2004, **42**, 1833–1839.
6. Gubernat, A., Stobierski, L. and Labaj, P., Microstructure and mechanical properties of silicon carbide pressureless sintered with oxide additives. *J. Eur. Ceram. Soc.*, 2007, **27**, 781–789.
7. Aoki, Y. and McEnaney, B., SiC foams produced by siliciding carbon foams. *Br. Ceram. Trans.*, 1995, **94**, 133–137.
8. Vignoles, G. L., Gaborieau, C., Delettrez, S., Chollon, G. and Langlais, F., Reinforced carbon foams prepared by chemical vapor infiltration: a process modeling approach. *Surf. Coat. Technol.*, 2008, **203**, 510–515.

9. Kaske, S. and Krawiec, P., Ordered mesoporous silicon carbide. *Stud. Surf. Sci. Catal.*, 2007, **170**, 1770–1773.
10. Lu, A. H., Schmidt, W., Kiefer, W. and Schüth, F., High surface area mesoporous SiC synthesized via nanocasting and carbothermal reduction process. *J. Mater. Sci.*, 2005, **40**, 5091–5093.
11. Sonnenburg, K., Adelhelm, P., Antonietti, M., Smarsly, B., Nöske, R. and Strauch, P., Synthesis and characterization of SiC materials with hierarchical porosity obtained by replication techniques. *Phys. Chem. Chem. Phys.*, 2006, **8**, 3561–3566.
12. Shiraishi, S., Kikuchi, A., Sugimoto, M. and Yoshikawa, M., Preparation of silicon carbide-based nanoporous materials by replica technique. *Chem. Lett.*, 2008, **37**, 574–575.
13. Qian, J. M., Wang, J. P., Jin, Z. H. and Qiao, G. J., Preparation of macroporous SiC and wood powder using infiltration-reaction process. *Mater. Sci. Eng. A*, 2003, **358**, 304–309.
14. Greil, P., Vogli, E., Fey, T., Bezold, A., Popovska, N., Gerhard, H. and Sieber, H., Effect of microstructure on the fracture behavior of biomorphous silicon carbide ceramics. *J. Eur. Ceram. Soc.*, 2002, **22**, 2697–2707.
15. Vogli, E., Mukerji, J., Hoffman, C., Kladny, R., Sieber, H. and Greil, P., Conversion of oak to cellular silicon carbide ceramic by gas-phase reaction with silicon monoxide. *J. Am. Ceram. Soc.*, 2001, **84**, 1236–1240.
16. Shin, D. W., Park, S. S., Choa, Y. H. and Niihara, K., Silicon/silicon carbide composites fabricated by infiltration of a silicon melt into charcoal. *J. Am. Ceram. Soc.*, 1999, **82**, 3251–3253.
18. Strecker, K. and Hoffmann, M. J., Effect of AlN-content on the microstructure and fracture toughness of hot-pressed and heat-treated LPS-SiC ceramics. *J. Eur. Ceram. Soc.*, 2005, **25**, 801–807.
19. Wu, Q. H. and Wu, J. A., *Introduction to polymer rheology*. China Chemical Industry Press, Beijing China, 1994.
20. Kearns. Process for preparing pitch foams. US Patent 5,868,974 (1999).
21. Neethling, S. J., Lee, H. T. and Grassia, P., The growth, drainage and breakdown of foams. *Colloids Surf. A*, 2005, **263**(1–3), 184–196.
22. Ness, J. N. and Page, T. F., Microstructural evolution in reaction-bonded silicon carbide. *J. Mater. Sci.*, 1986, **21**, 1377–1397.
23. Zangvil, A. and Ruh, R., Phase relationship in the silicon carbide-aluminum nitride system. *J. Am. Ceram. Soc.*, 1988, **71**, 884–890.
24. Brezny, R., Green, D. J. and Dam, C. Q., Evaluation of strut strength in open-cell ceramics. *J. Am. Ceram. Soc.*, 1989, **72**, 885–889.
25. Gibson, L. J. and Ashby, M. F., *Cellular solids: structure and properties* (*second edition*). Cambridge University Press, Cambridge, UK, 1997, pp. 175–231.
26. Kingery, W. D., Factors affecting thermal stress resistance of ceramic materials. *J. Am. Ceram. Soc.*, 1955, **38**, 3–15.